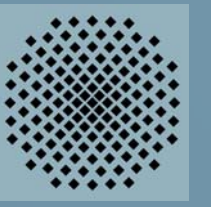




Similarity characterization of short-term aftershocks generated by the Feb 11th 2004 Northern Dead Sea (M_L 5.1) earthquake



Universität Stuttgart

¹ Dep. of Geophysics & Planetary Sciences
Tel Aviv University
Tel-Aviv 69978
Israel

Wust-Bloch ¹, G. H., and Joswig ², M.

Hillel@seismo.tau.ac.il
Joswig@geophys.uni-stuttgart.de

² Institut für Geophysik
Universität Stuttgart
D-70174 Stuttgart
Germany

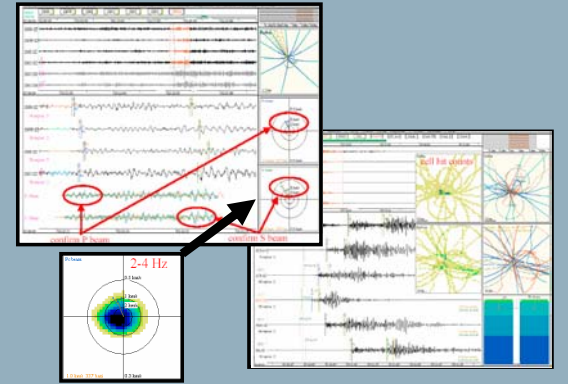
Data acquisition & processing



Data acquisition

SNS [Seismic Navigation System] consists of three single-component short-period seismometers (Lennartz Le-1D) arranged as tripartite array around one central three-component short-period sensor (Lennartz Le-3D). Data detected by this six-channel SNS is acquired by a 24 bit digitizer (*Orion-6* by Nanometrics, *M-24/6* by Lennartz). The array aperture varies as a function of the monitoring tasks, source remoteness and field constrains. For applications in earthquake seismology, an array aperture of 50 to 100 m is optimal.

The concept of nanoseismic monitoring (Joswig, 2005) was developed to detect, characterize and locate sources of seismic energy generated at distances between 10 m and 10 km and with magnitudes down to M_L -4.0 (Wust-Bloch and Joswig, 2006). It was designed with the idea that ultimate instrumental portability optimizes SNR conditions by minimizing source-to-sensor distance and allows immediate instrument deployment with minimal logistical constraints. Nanoseismic monitoring integrates data acquisition by SNS [Seismic Navigation Systems] (see left) and data analysis by SparseNet software (Joswig, 1999) (see right).



Data processing

Nanoseismic monitoring is an application of passive seismic field investigations tuned to ultimate sensitivity. It integrates innovative approaches in signal processing (Joswig, 1996; 1999; 2000 & in review) whereby pattern recognition schemes and automated sonogram-based waveform analysis lowers the processing threshold to near 0 dB SNR. By displaying and updating simultaneously the data uncertainty of this over-determined system, *HypoLine* software allows the operator to slide through parameter space, observing in real-time the effect of each parameter change on the solution (Joswig, in review).

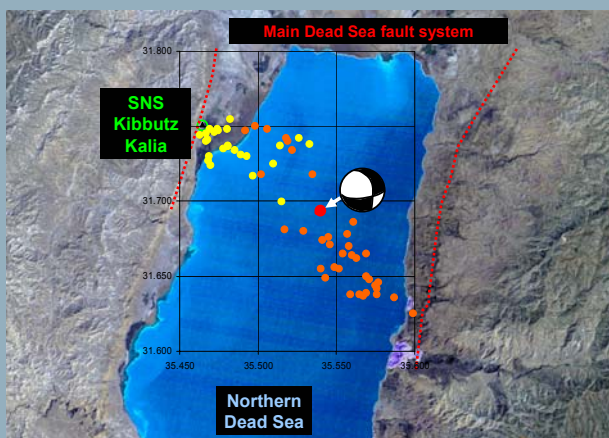


Fig. 1. Mainshock and aftershock locations with location of recording SNS and main Dead Sea fault system (dotted red)

1. The February 11th 2004 (M_L 5.1) Dead Sea Earthquake

One SNS [Seismic Navigation System], deployed less than five hours after the main shock, recorded a series of 61 aftershocks ($-2.0 < M_L < 2.4$) within 17 hours. The aftershocks cluster (Figure 1) within an E-W trending and south-dipping discontinuity zone, which is consistent with available fault plane solutions and supports a new tectonic model for the Northern Dead Sea basin (Lazar et al., 2006). The location of the SNS (Figure 1), which was accidentally deployed on top of the main western boundary fault of the Dead Sea fault system (red dotted line), resulted in part of the seismic energy being guided by the dominant Dead Sea structure (Gottschämmer et al., 2005; Gottschämmer et al., 2002; Wust-Bloch, 2002) and raised the complexity of data processing.

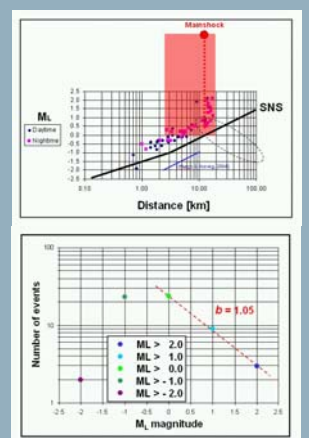


Fig. 2. Instrumental sensitivity of recording SNS and catalogue completeness (b -value) for events above $M_L > 0.0$

2. Instrumental sensitivity & catalogue completeness

The event detection threshold (Figure 2a) confirms that the location of aftershocks stronger than $M_L > 0.0$ (red band) is unbiased by instrument sensitivity within a radius of at least 15 km. Characterization of short-term seismicity (Figure 2b) yields an elevated (1.05) b -value and confirms that the event catalog is indeed complete down to 0.0 M_L .

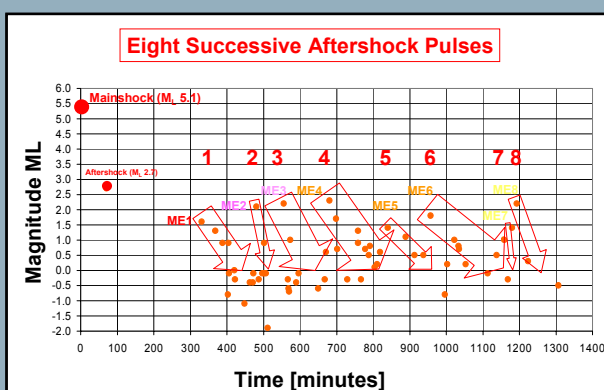


Fig. 3. Time distribution of aftershocks energy (M_L) locations with location of recording SNS and main Dead Sea fault system (dotted red)

3. Time distribution of aftershock energy (M_L)

During the 17-hour monitoring period (300-1320 min), no regular and stable event magnitude decay can be observed. The non-random event distribution (Figure 3) shows that each of the eight stronger ($M_L > 1.4$) aftershocks (ME1 to ME8) is followed by varying series of sub-events with rapidly decreasing magnitudes. They are characterized by an initial magnitude drop of about one order, a standard feature of aftershocks (Utsu, 1971).

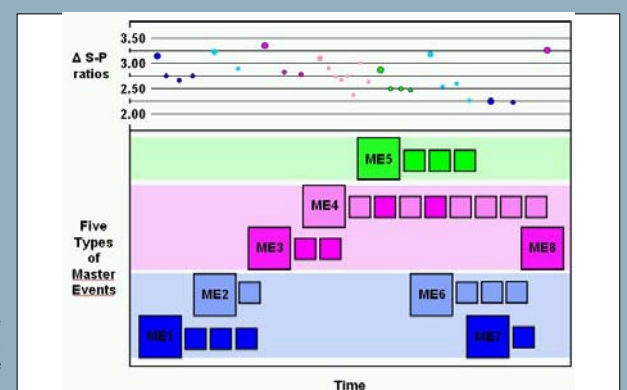


Fig. 4. Waveform classification and Δ S-P ratios for $M_L > 0.0$ events

4. Event similarity & Δ S-P ratios

Waveform classification of $M_L > 0.0$ events according to five generic master event (ME) patterns. This time classification correlates with M_L -time decay (Figure 3) and with time variation of Δ S-P ratios (see top Figure 4).

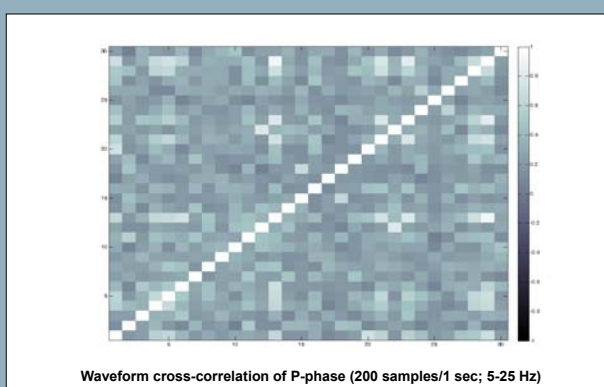


Fig. 5. Waveform cross-correlation test

5 & 6 Waveform cross-correlation and Dendrogram

A waveform cross-correlation and a dendrogram test was carried out for the P -phases of $M_L > 0.0$ events on the 5-25 Hz band (Haeg, in prep). The low correlation observed on both diagrams (Figures 5 & 6.) can be related to the fact that, in this case, waveforms are sensitive to interacting factors such as:

- Wave-guiding by the Dead Sea western boundary fault system (see Figure 1)
- Location of the array sensors within the axis of the main fault system (see Figure 1).

These investigations show that a simple sonogram-based waveform classification (Figure 4) offer a better correlation with the time distribution of M_L and Δ S-P ratios.

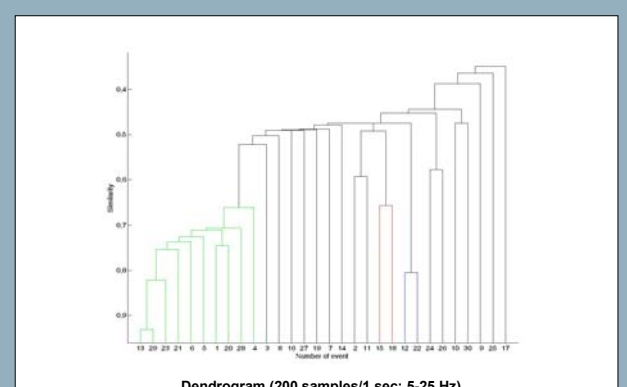


Fig. 6. Dendrogram test